Karson, J.A., Cannat, M., Miller, D.J., and Elthon, D. (Eds.), 1997
Proceedings of the Ocean Drilling Program, Scientific Results, Vol. 153

19. PETROLOGY AND GEOCHEMISTRY OF CROSSCUTTING DIABASE DIKES, SITES 920 AND 921[1]

Pamela D. Kempton[2] and John F. Casey[3]

ABSTRACT

New major-element, trace-element, and Sr-, Nd-, Pb-, and O-isotope data are presented for <0.75-m.y.-old diabase dikes recovered during Leg 153. Diabase dikes encountered at Site 920 have MgO contents ranging from 13 to 15 wt%, along with high Ni and Cr and low concentrations of most incompatible trace elements. However, concentrations of most major elements and some mobile trace elements have been strongly modified by hydrothermal alteration, leading to enrichment in MgO and Sr, and to depletions in CaO, FeO, and TiO_2. Sr isotopes indicate that the fluids responsible for alteration of the diabase at Site 920 had low $^{87}Sr/^{86}Sr$ compared with seawater; these low values are thought to be typical of the fluid composition during the earliest stages of alteration, not only of the diabase dikes, but also of the peridotite section they crosscut. Depletion in ^{18}O (+4.9 to +5.2‰) relative to average mid-ocean ridge basalt (MORB) is consistent with hydrothermal alteration involving seawater at moderate temperatures (250°–300°C).

Estimates of the original composition of the Site 920 diabase before alteration suggest they contained ~11 wt% MgO and were remarkably similar to the primary melt compositions proposed by Sullivan (1991) for the Mid-Atlantic Ridge south of the Kane Fracture Zone (MARK) area. In contrast, diabase dikes at Site 921 are similar in composition to recent MARK basalts (MgO ~8 wt%), but have slightly higher CaO and Al_2O_3 and lower incompatible trace-element contents at a given MgO.

Trace-element modeling is consistent with the diabase from Site 920 being generated as a pooled melt by <15% melting of mantle peridotite in the spinel facies (i.e., shallow depths of melting). Recent MARK basalts and diabase from Site 921 were generated by slightly larger degrees of melting. Lower $^{143}Nd/^{144}Nd$ ratios (0.51313) and flatter REE patterns (Ce/Yb = ~1) are consistent with a less-depleted source for the Site 920 diabase than for that giving rise to the majority of MARK gabbros (0.51318–0.51322) and recent MARK basalts (0.51314–0.51318; Ce/Yb = 0.9). The average isotopic composition of the mantle source supplying the MARK magma system has changed over a period of <1 m.y., becoming more radiogenic in Pb, but less radiogenic in its Nd-isotope composition with time. This indicates that, on average, the present mantle source is less depleted than that ~750,000 yr earlier. However, the contemporaneity of rocks derived from relatively depleted sources (i.e., Sites 921–924 gabbros and Site 921 dikes) and those from significantly less depleted sources (i.e., Site 920 diabase and amphibolitized microgabbro) supports a mixing model in which the proportion of enriched to depleted mantle components changes with time, rather than a gradual compositional shift of a homogeneous source.

INTRODUCTION

Basalts from the Mid-Atlantic Ridge south of the Kane Fracture Zone (MARK) area are characterized by a limited range of compositions (Reynolds, 1995; Bryan et al., 1994; Dosso et al., 1993), with a relatively evolved basalt being the most abundant type (Bryan et al., 1981). Yet, diabase dikes encountered during Ocean Drilling Program Leg 153 include some of the most Mg-rich compositions from the MARK area reported to date. These unusual Mg-rich compositions are usually only observed as melt inclusions in phenocrysts (Sobolev and Shimizu, 1993), and could be representative of the primary magma compositions supplying the magma system at MARK. In this paper we present new major-element, trace-element, and Sr-, Nd-, Pb-, and O-isotope data for diabase dikes recovered during Leg 153, and offer some preliminary observations and interpretations regarding their petrogenesis.

The MARK area is characterized by slow-spreading rates and basalt compositions that are typical of normal mid-ocean ridge basalts away from the influence of hotspot plumes (N-MORB). The area is divided into two distinct ridge segments that have contrasting deep crustal structures. The northern segment extends from the nodal basin to 23°18′N and has a seismic crustal thickness of 4–5 km. A prominent neovolcanic ridge in this segment appears to be a relatively young fissure eruption; the associated lavas are among the most geochemically primitive in the MARK area (Bryan et al., 1994). The active Snake Pit hydrothermal field is associated with this feature. In contrast, the southern segment has a seismic crustal thickness of 6–7 km (Purdy and Detrick, 1986), and consists of older, more fissured terrain that shows no evidence for recent hydrothermal or volcanic activity. Instead, basalts from the southern segment appear to represent the last stages of an older eruptive event (Bryan et al., 1994). A broad transition zone of significantly thinner crust separates the two domains, and has been interpreted as a zero-offset transform fault (Purdy and Detrick, 1986) or an "accommodation zone" (Karson, 1991).

Coarse-grained mafic and ultramafic rocks, believed to be approximately 0.75 m.y. old, are exposed along the western wall of the median valley at MARK and were drilled during Leg 153. Peridotite was recovered at Site 920; gabbro was recovered at Sites 921–924. The gabbro sites are located approximately in the middle of the northern segment, whereas the peridotite site is located near the offset of the northern and southern spreading segments at 23°21′N. Diabase dikes were encountered crosscutting the peridotite in Holes 920B and 920D and crosscutting the gabbro section in Holes 921B and 921C. This paper investigates the relationship of these dikes (1) to each other, (2) to the peridotite and gabbro sections they crosscut, and (3) to recent volcanism in the axial valley.

PETROGRAPHY

The primary and secondary petrographic characteristics of the diabase dikes recovered during Leg 153 are described in detail in Cannat, Karson, Miller, et al. (1995). Only a brief summary is provided

[1]Karson, J.A., Cannat, M., Miller, D.J., and Elthon, D. (Eds.), 1997. *Proc. ODP, Sci. Results,* 153: College Station, TX (Ocean Drilling Program).

[2]NERC Isotope Geosciences Laboratory, Kingsley Durham Centre, Keyworth, NG12 5GG, United Kingdom. P.KEMPTON@NIGL.NERC.AC.UK

[3]Department of Geosciences, University of Houston, Houston, TX 77204, U.S.A.

below; the reader is referred to Cannat, Karson, Miller, et al. (1995) for further details.

Site 920—Diabase Crosscutting Peridotite

Diabase recovered from Site 920 is moderately phyric (olivine + plagioclase) basalt. Although contacts with the surrounding peridotite were not recovered, the diabase is thought to be intrusive into the peridotite because it is finer grained and contains fewer phenocrysts at the top and bottom of its occurrence in Hole 920D, and is aphyric at the top of its occurrence in Hole 920B. The dike is inferred to be about 3.5–4 m thick (Shipboard Scientific Party, 1995).

The diabase has a porphyritic intergranular to subophitic texture and contains tabular plagioclase (0%–10%) phenocrysts and euhedral pseudomorphs after olivine (0%–10%). Some olivine pseudomorphs are skeletal in shape and contain euhedral Cr spinels. The groundmass is composed of fine-grained plagioclase, clinopyroxene, olivine, and opaque iron oxide minerals in a smectite-chlorite matrix. Modes for original igneous groundmass minerals are difficult to determine because of the extent of alteration, but they are estimated to have been ~55% plagioclase, 25% olivine, and 20% clinopyroxene.

The diabase from Site 920 is moderately to highly altered, consisting predominantly of clay minerals and chlorite after groundmass mesostasis, plagioclase, and olivine. Ca-plagioclase (An_{73}) is replaced by a more Na-rich plagioclase (An_{14}); other alteration minerals after plagioclase include minor amounts of epidote, prehnite, and zeolites. Clinopyroxene is partially replaced by pale-green amphibole and chlorite. Total alteration is visually estimated at 30%–50% of the mode.

Site 921—Diabase Crosscutting Gabbro

Moderately phyric to aphyric diabase was recovered from Site 921. Igneous contacts with the gabbroic country rock were recovered only from the top contact of diabase in Hole 921B. The diabase from the chilled margin contains plagioclase phenocrysts (up to 3.5 mm) and chlorite pseudomorphs after olivine. Some plagioclase phenocrysts contain spinel inclusions. Away from the chilled margin, the groundmass is intergranular and consists of a fine-grained aggregate of plagioclase (~48%), clinopyroxene (~45%), olivine (5%), and iron oxide minerals (2%).

Groundmass olivine and portions of the intergranular groundmass are altered to chlorite and clay minerals. Sulfides typically line the grain boundaries of the altered olivines. Plagioclase phenocrysts are partly replaced by clay minerals, but clinopyroxene is relatively fresh throughout; locally it is rimmed by chlorite and actinolite. Total alteration is visually estimated at 10%–20%.

Analytical Techniques

Before crushing and isotopic analysis, all samples were washed in deionized (Milli-Q brand) water in an ultrasonic bath to remove any surface contaminants that might be acquired through handling or drilling. Whole-rock powders were leached before dissolution, using either 1.5-M HCl for 30 min on a hot plate at ~100°C, followed by leaching in hot 6-M HCl for ~30 min, or hot 6-M HCl alone for 30 min. The leachates were removed sequentially, and the residue rinsed in Milli-Q H_2O. The 6-M HCl leachates and the final Milli-Q H_2O rinses were combined and processed together for isotopic analysis. Whole-rock powders were also analyzed in unleached form for comparative purposes. Details of the chemical procedures used for isotope analysis are given in Kempton and Hunter (this volume). Sr, Pb, and Nd were run as the metal species on single Ta, single Re, and double Re-Ta filaments, respectively, using a Finnegan MAT 262 multicollector mass spectrometer in static mode at the NERC Isotope Geosciences Laboratory (NIGL). Blanks for Sr, Nd, and Pb were less than 500 pg, 800 pg, and 250 pg, respectively. $^{87}Sr/^{86}Sr$ was normalized at run time to $^{86}Sr/^{88}Sr = 0.1194$; $^{143}Nd/^{144}Nd$ was normalized to a value of $^{146}Nd/^{144}Nd = 0.7219$. Samples for this and related studies were analyzed over a period of 18 months, so in order to minimize the effects of machine drift, sample results are further normalized to accepted values for NBS 987 (National Bureau of Standards) and J&M (Johnson and Matthey) of 0.71024 and 0.51111, respectively. Minimum uncertainties are derived from external precision of standard measurements, which average 27 ppm for $^{143}Nd/^{144}Nd$ and 18 ppm for $^{87}Sr/^{86}Sr$. Based on repeated runs of NBS 981, the reproducibility of Pb-isotope measurements is better than ±0.1% per a.m.u. Pb-isotope ratios have been corrected relative to the average standard Pb-isotopic compositions of Todt et al. (1984).

Ratios of $^{18}O/^{16}O$ were also determined at NIGL. Details of sample analysis technique can be found in Kempton and Hunter (this volume). All final $^{18}O/^{16}O$ ratios have been reported as δ values in per mil (‰), relative to the standard mean oceanic water (SMOW) standard of Craig (1961). All results are normalized to the accepted value for the international standard XRC (Glendessary pyroxenite, i.e., +6.6‰); this sample was run with each batch of analyses (average value $+6.2 \pm 0.4$‰; $n = 25$, 2σ).

Major-, trace-, and rare-earth-element (REE) analyses were conducted using inductively coupled plasma atomic emission spectroscopy (ICP-AES) at the University of Houston and augmented by shipboard data for some of the samples. Analytical techniques are discussed in Casey (this volume).

RESULTS

Major and Trace Elements

Major-element data are presented in Table 1 and shown graphically in Figures 1 and 2. Most of the basalts from the MARK area are characterized by remarkably little chemical variation (Reynolds, 1995; Dosso et al., 1993; Bryan et al., 1994; J.F. Casey, unpubl. data). On plots of MgO vs. oxide concentrations, the recent axial basalts tend to form tight clusters or linear arrays (Figs. 1A–1E). The diabase dikes from Site 921 are compositionally similar to recent MARK basalts, but they are distinguished by having higher Al_2O_3 and CaO, and lower Na_2O for a given MgO. In contrast, although the diabase dikes from Site 920 form linear trends on all MgO vs. oxide plots, the trends are oblique to those formed by the recent MARK basalts. The primitive magma composition for the MARK area calculated from the compositions of melt inclusions in phenocrysts (Sullivan, 1991) lies not only on the Site 920 diabase dike trend, but also on an extension of the recent MARK basalt trend (i.e., at or near the intersection of the two).

Figure 1F shows the variation in MgO vs. Ni. In contrast to the MgO vs. oxide plots, the diabase dikes from Site 920 exhibit a similar trend to that formed by the recent MARK basalts, but at Ni contents that are at least twice those of the most primitive MARK basalts reported to date. Cr contents are similarly high (Table 1).

Trace-element results are summarized in a chondrite-normalized incompatible-element plot (Fig. 2). Again, the range of compositions from recent MARK basalts (Reynolds, 1995; J.F. Casey, unpubl. data) is shown for comparison. The diabase samples from Site 921 lie near the middle of the range of compositions of recent MARK basalts, but they are clearly less depleted in Ba. The dike samples from Site 920 lie within the range of recent MARK basalts for most elements, but they have among the lowest concentrations for elements to the right of Nd (i.e., elements less incompatible); elements to the left of Nd (i.e., more incompatible) either plot above or near the middle of the field of recent MARK basalts. Most distinctive is the strong positive Sr anomaly, which corresponds to an enrichment in Sr of more than three times that expected on the basis of elements with similar incompatibility (i.e., Ce and Nd). The REE patterns indicate that the Site 920 dike samples are very slightly less depleted than recent MARK basalts ($Ce_N/Yb_N = \sim 1.00$ as opposed to ~0.92 for the re-

Table 1. Major- and trace-element data for diabase dikes at Sites 920 and 921.

Hole, core, section:	920B-9R-3	920B-9R-4	920D-8R-3	920D-8R-3	920D-10R-1	921B-1W-2	921C-2R-1
Interval (cm):	55–57	17–20	66–73	80–85	57–60	5–8	3–7
SiO_2	46.64	48.25	48.10	48.90	50.21	49.08	50.19
TiO_2	1.04	0.91	0.99	0.96	1.11	1.38	1.31
Al_2O_3	18.05	17.47	16.68	18.27	14.93	16.96	16.89
Fe_2O_3	9.00	8.62	8.86	8.82	9.55	9.39	9.49
MnO	0.25	0.16	0.25	0.23	0.28	0.18	0.15
MgO	13.03	12.14	14.00	12.74	15.08	7.99	7.61
CaO	8.92	9.58	7.73	8.44	6.21	11.86	11.80
Na_2O	2.20	2.81	2.70	2.91	3.36	2.58	2.69
K_2O	0.01	0.02	0.02	0.05	0.02	0.01	0.02
P_2O_5	0.05	0.05	0.04	0.08	0.04	0.08	0.07
Total	99.19	100.01	99.37	101.51	100.79	99.51	100.22
LOI	4.29	3.61	4.49	4.01	4.58	1.93	1.41
CO_2	0.00		0.04		0.06	0.01	0.00
H_2O	5.87		5.75		5.71	2.57	2.19
Mg#	74.14	73.61	75.78	74.55	75.77	62.76	61.36
V	**214**	**153.65**	**177.01**	**151.62**	**177.72**	**202.57**	**217.83**
Ti			**5708.1**		**5952.9**	**7576.9**	**7631.2**
Cr	**391**	**469.19**	**426.8**	**473.47**	**489.12**	**274.33**	**280.48**
Ni	**228**	**272.5**	**276.82**	**250.73**	**280.68**	**117.86**	**122.23**
Co			**44.26**		**46.54**	**54.22**	**55.08**
Cu			**11.64**		**0.97**	**61.67**	**73.76**
Zn			**70.10**		**93.54**	**50.29**	**55.74**
Sr	**190**	**339.79**	**286.65**	**334.17**	**300.40**	**131.23**	**137.05**
Zr	**70**	**68.80**	**69.08**	**71.66**	**74.97**	**88.90**	**86.92**
Ba	**1**	**54.72**	**16.74**	**19.60**	**22.52**	**13.27**	**14.42**
Nb	*1*		*1*		*1*		
Rb	*1*		*0*		*1*	*1*	*1*
Zn	*97*		*71*		*106*	*61*	*58*
Cu	*16*		*11*		*6*	*72*	*76*
Sc		**30.19**	**31.13**	**31.58**	**33.83**	**36.26**	**35.32**
Y		**21.47**	**21.23**	**22.7**	**23.97**	**29.83**	**29.84**
La		**2.06**	**5.08**	**2.53**	**2.7**	**2.72**	**3.03**
Ce		**7.3**	**7.82**	**8.79**	**8.52**	**9.69**	**9.73**
Nd		**6.15**	**6.36**	**6.59**	**6.66**	**8.86**	**8.84**
Sm		**1.91**	**2.04**	**2.16**	**2.22**	**2.95**	**2.92**
Eu		**0.76**	**0.74**	**0.84**	**0.93**	**1.21**	**1.19**
Gd		**2.44**	**2.68**	**2.92**	**3.04**	**4.03**	**3.97**
Dy		**3.31**	**3.33**	**3.56**	**3.7**	**4.83**	**4.69**
Er		**2.11**	**2.28**	**2.32**	**2.4**	**3.04**	**2.99**
Yb		**2.01**	**2.05**	**2.21**	**2.35**	**2.77**	**2.77**
Lu		**0.29**	**0.34**		**0.39**	**0.44**	**0.44**
Zr/Sm		36.02	33.86	33.18	33.77	30.14	29.77
Zr/Y		3.20	3.25	3.16	3.13	2.98	2.91

Notes: Mg numbers were calculated as $Mg/(Mg+Fe^{tot}) * 100$. Trace elements in bold were determined by ICP; trace elements in italics were determined by XRF. LOI = loss on ignition.

cent MARK basalts); heavy REE contents are among the lowest and lie outside the field of MARK basalts reported by Reynolds (1995), whereas Ce concentrations lie within the field of MARK. La concentrations show a wide range in Site 920 diabase samples; duplication of these results on repeat analysis indicates that this range is not due to analytical problems. It is probably the result of La mobility during alteration. Similar mobility during alteration has been noted in MARK basalts between palagonite pillow rims and cores (Ludden and Thompson, 1977) and elsewhere (Menzies et al., 1977; Sparks, 1995).

Isotopes

Results of isotopic analysis are listed in Table 2 and shown graphically in Figures 3 and 4. Considered collectively, there is a relatively wide range of Sr- and Nd-isotope values for the samples analyzed from the MARK area, but the different lithologic groups cluster into more restricted compositional ranges. Massif gabbros from Sites 921 to 924 have relatively high Nd- and low Sr-isotope values. Gabbroic dikes from Site 920 have similar Nd-isotope compositions to massif gabbros from Sites 921 to 924, but significantly higher $^{87}Sr/^{86}Sr$ ratios (Kempton and Hunter, this volume). Diabase dikes that crosscut the massif gabbros in Holes 921B and 921C are isotopically similar to the massif gabbros; both lie toward the depleted end of the field for North Atlantic N-MORB, but have slightly lower Nd-isotope ratios than reported by Machado et al. (1982) for samples dredged from the southern wall of the Kane Fracture Zone approximately 5 km to the north. Note that the Machado et al. (1982) values are higher than most other reported values for the North Atlantic MORB; only two unusual samples from 17°N (Dosso et al., 1993) have higher $^{143}Nd/^{144}Nd$ values. We have analyzed plagiogranite and diabase (P.D. Kempton, unpubl. data) dredged from localities near those analyzed by Machado et al. (1982), and these samples yield Nd-isotope values identical to those of Leg 153 gabbros. We therefore suspect that there is an interlaboratory bias, and that the Machado et al. (1982) data may need revision to be internally consistent with our own data.

Recent basalts from the neovolcanic zone have low $^{87}Sr/^{86}Sr$, similar to the massif gabbros and diabase dikes from Site 921 (Fig. 3), but they have overlapping to lower $^{143}Nd/^{144}Nd$ ratios (Kempton and Hunter, this volume; Dosso et al., 1993). Off-axis basalts exhibit a similar range in Nd-isotope values, but extend to higher $^{87}Sr/^{86}Sr$ ratios, presumably as a result of seawater alteration. The diabase dikes from Site 920 are isotopically distinct, having higher $^{87}Sr/^{86}Sr$ and lower Nd-isotope values than both recent basalts and massif gabbros from Sites 921 to 924.

Pyroxenes separated from Site 920 ultramafic peridotites have the most depleted Nd-isotope signatures found within the MARK area to date (Kempton and Stephens, this volume) and overlap the high end of the range of values reported for North Atlantic MORB. The high Sr-isotope compositions clearly indicate seawater alteration, and it is

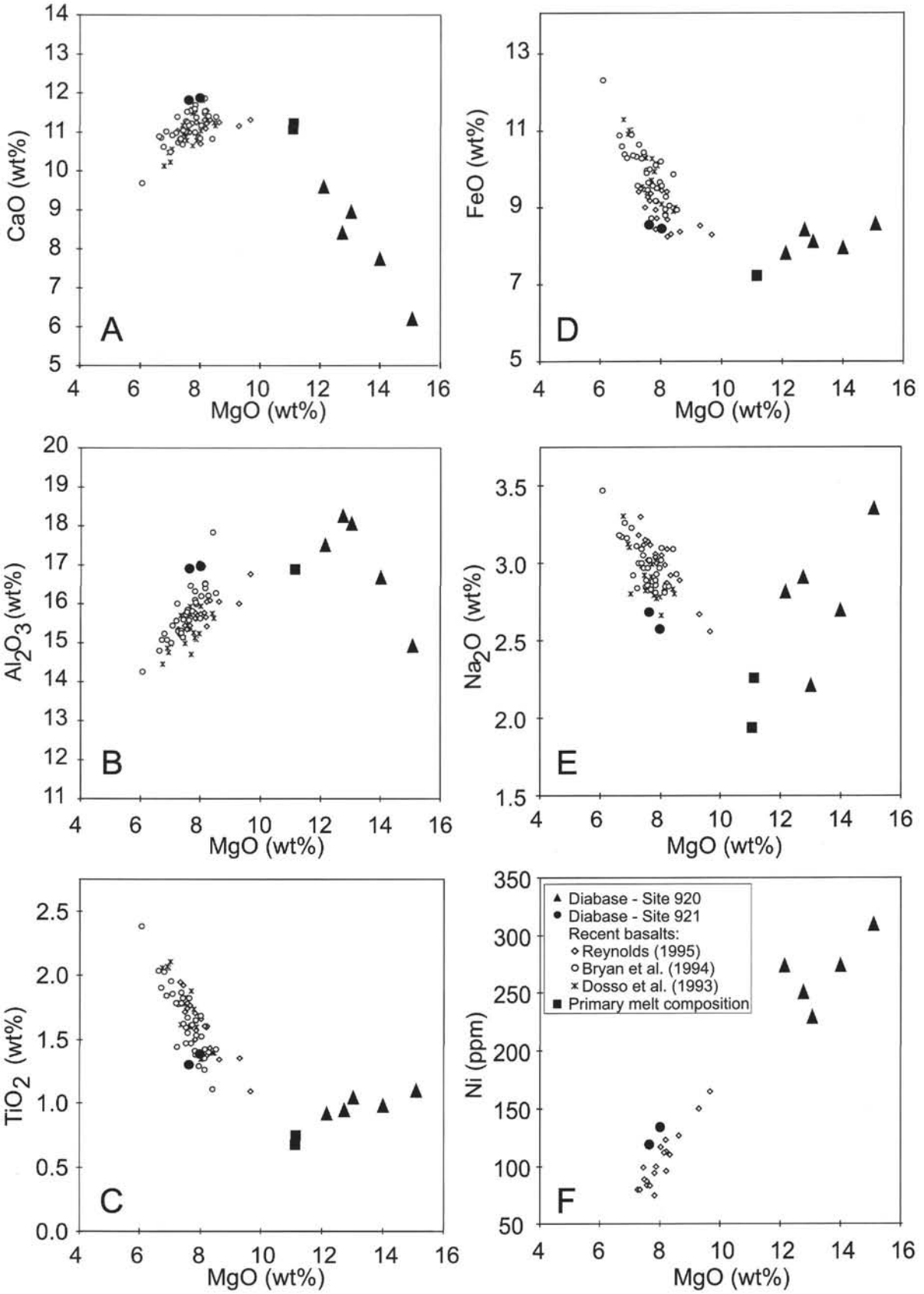

Figure 1. Plot of MgO vs. oxide (wt%) or elemental (ppm) concentration of **(A)** CaO, **(B)** Al_2O_3, **(C)** TiO_2, **(D)** FeO, **(E)** Na_2O, and **(F)** Ni for diabase dikes from Sites 920 and 921. Data for recent axial basalts from Reynolds (1995), Bryan et al. (1994), and Dosso et al. (1993). Primary melt compositions are from Sullivan (1991).

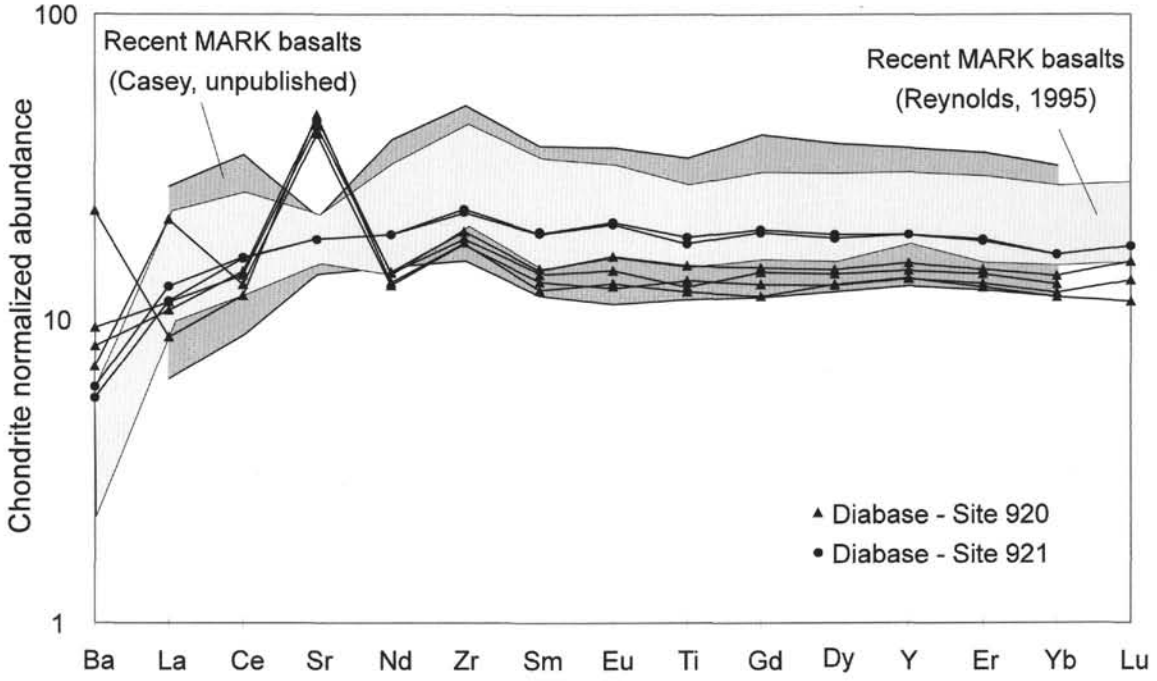

Figure 2. Chondrite-normalized, extended, incompatible trace-element plot. Normalizing values are from Sun and McDonough (1989). The field for recent MARK basalts (J.F. Casey, unpubl. data) excludes some unusual high-Al basalts from an older uplifted fault block; Ba and Lu are also not available for this data set. See text for discussion.

Table 2. Sr, Nd, and Pb isotopes from diabase dikes.

Core, section, interval (cm)		Type	$^{87}Sr/^{86}Sr$	$^{87}Sr/^{86}Sr$ average	$^{143}Nd/^{144}Nd$	$^{143}Nd/^{144}Nd$ average	$^{206}Pb/^{204}Pb$	$^{207}Pb/^{204}Pb$	$^{208}Pb/^{204}Pb$	$^{206}Pb/^{204}Pb$ average	$^{207}Pb/^{204}Pb$ average	$^{208}Pb/^{204}Pb$ average	$\delta^{18}O$
153-920B-													
9R-3, 95–101	(1A)	LR	0.703296	0.703282	0.513129	0.513136	18.376	15.505	37.850	18.376	15.505	37.850	+4.8
9R-3, 95–101	(2A)	LR	0.703268		0.513144								
9R-3, 95–101	(1A)	UL	0.703201	0.703212	0.513130	0.513138	18.386	15.521	38.005	18.413	15.551	38.088	
9R-3, 95–101	(2A)	UL	0.703223		0.513146		18.440	15.580	38.170				
9R-3, 95–101	(2A)	LL*	0.703071	0.703071	0.513143	0.513143	18.449	15.601	38.309	18.449	15.601	38.309	
9R-3, 95–101	(1A)	LL	0.702696	0.702668	0.513136	0.513130	18.437	15.576	38.242	18.461	15.604	38.339	
9R-3, 95–101	(1B)	LL	0.702693										
9R-3, 95–101	(2A)	LL	0.702615		0.513125		18.486	15.631	38.437				
153-920D-													
9R-2, 128–134	(1A)	LR	0.703371	0.703346		0.513143	18.374	15.494	37.803	18.386	15.512	37.854	+4.9
9R-2, 128–134	(2A)	LR	0.703358		0.513143		18.398	15.529	37.906				
9R-2, 128–134	(1A)	UL	0.703285	0.703307		0.513131	18.441	15.535	38.044	18.455	15.552	38.085	
9R-2, 128–134	(2A)	UL	0.703328		0.513131		18.469	15.568	38.127				
9R-2, 128–134	(2A)	LL*	0.703347	0.703347	0.513106	0.513106	18.544	15.604	38.343	18.544	15.604	38.343	
9R-2, 128–134	(1A)	LL	0.702732	0.702736	0.513124	0.513124	18.500	15.579	38.219	18.530	15.606	38.311	
9R-2, 128–134	(1B)	LL	0.702714										
9R-2, 128–134	(2A)	LL	0.702761		0.513125		18.561	15.634	38.404				
153-921B-													
1W-2, 0–5	(1A)	LR	0.702410	0.702402	0.513192	0.513189	18.151	15.471	37.594	18.169	15.491	37.648	+4.7
1W-2, 0–5	(2A)	LR	0.702394		0.513186		18.187	15.511	37.703				
1W-2, 0–5	(1A)	UL	0.702400	0.702415		0.513197	18.237	15.501	37.787	18.252	15.516	37.826	
1W-2, 0–5	(2A)	UL	0.702429		0.513197		18.267	15.531	37.865				
1W-2, 0–5	(2A)	LL*	0.702886	0.702886	0.513190	0.513190	18.330	15.560	38.041	18.330	15.560	38.041	
1W-2, 0–5	(1A)	LL	0.702538	0.702505	0.513184	0.513194	18.256	15.501	37.822	18.262	15.516	37.853	
1W-2, 0–5	(1B)	LL	0.702533		0.513198								
1W-2, 0–5	(2A)	LL	0.702445		0.513200		18.267	15.530	37.884				
153-921C-													
92R-1, 29–34	(1A)	LR	0.702399	0.702391	0.513214	0.513210	18.132	15.465	37.544	18.148	15.485	37.588	+5.2
92R-1, 29–34	(2A)	LR	0.702383		0.513206		18.165	15.504	37.632				
92R-1, 29–34	(1A)	UL	0.702470	0.702442	0.513195	0.513190	18.182	15.485	37.673	18.199	15.506	37.738	
92R-1, 29–34	(1B)	UL	0.702421										
92R-1, 29–34	(2A)	UL	0.702433		0.513185		18.216	15.527	37.804				
92R-1, 29–34	(2A)	LL*	0.703000	0.703000	0.513182	0.513182	18.246	15.533	37.875	18.246	15.533	37.875	
92R-1, 29–34	(1A)	LL	0.702594	0.702552	0.513207	0.513193	18.204	15.487	37.699	18.204	15.495	37.721	
92R-1, 29–34	(1B)	LL	0.702576		0.513200								
92R-1, 29–34	(2A)	LL	0.702485		0.513173		18.204	15.503	37.743				

Notes: Abbreviations as follows: LR = leached residue, LL = leachate, UL = unleached; * = 1.5-M HCl leach (all other leachates are 6-M HCl). Numbers in parentheses after sample name indicate sample split and order of dissolution (i.e., 1 = first dissolution of the sample, 2 = same sample but a completely new dissolution). Letters indicate order of multiple analyses from the sample dissolution.

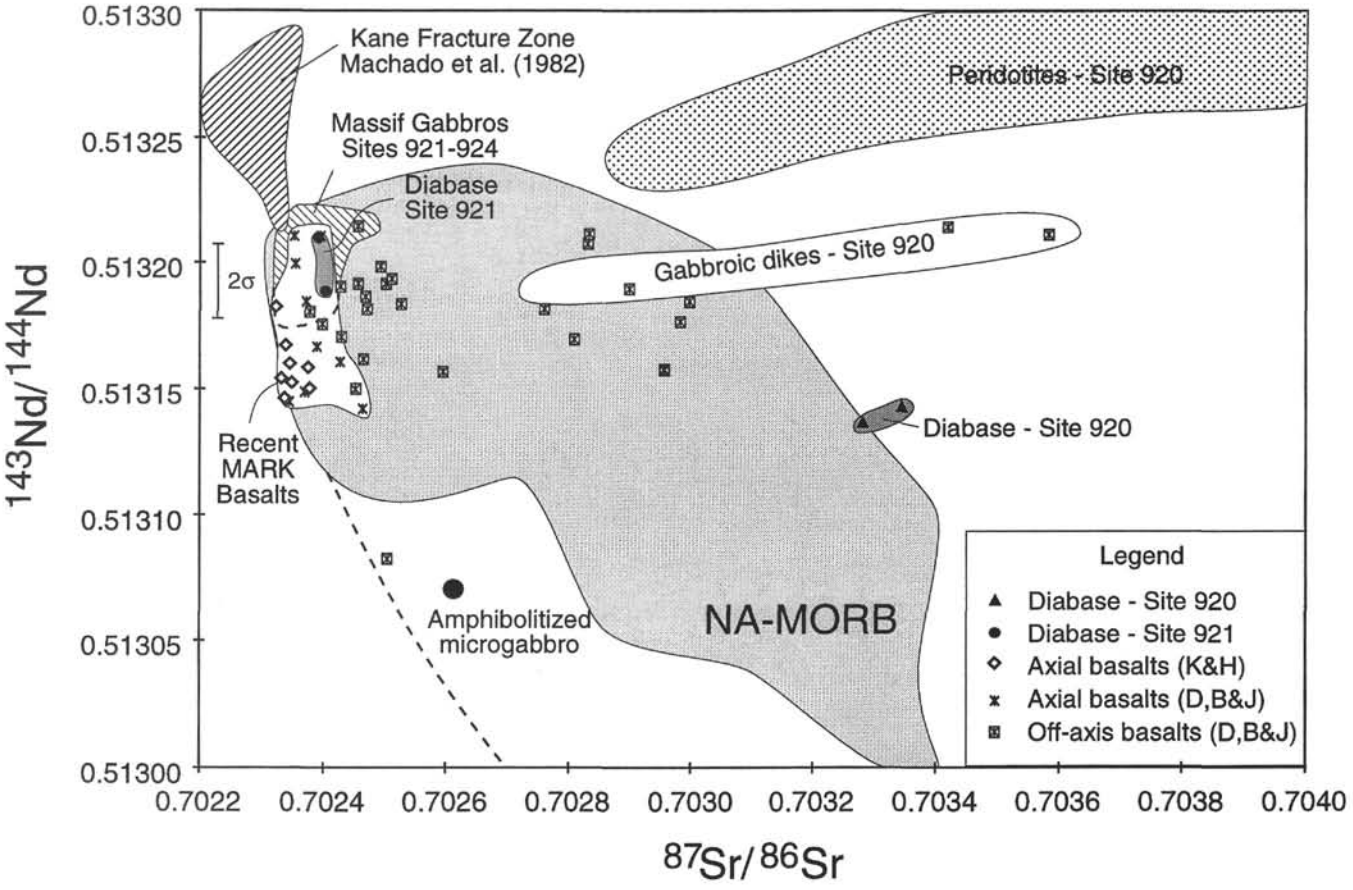

Figure 3. Plot of $^{87}Sr/^{86}Sr$ vs. $^{143}Nd/^{144}Nd$ for Leg 153 diabase dikes; data plotted are average values of leached residues from Table 2. Shown for comparison are fields for peridotites from Site 920 (Kempton and Stephens, this volume), gabbros from Sites 920 and 921, amphibolitized microgabbro from Site 920, recent MARK basalt glasses from the neovolcanic zone (open diamonds = Kempton and Hunter, this volume; asterisk = Dosso et al., 1993), off-axis MARK basalts (crossed squares = Dosso et al., 1993), and North Atlantic N-MORB (indicated as NA-MORB on figure). Data for NA-MORB field from Cohen et al. (1980), Cohen and O'Nions (1982), Dosso et al. (1993), Frey et al. (1993), Ito et al. (1987), White and Hofmann (1982). Data from Machado et al. (1982) are shown separately; these data have been normalized using Machado's published value for international rock standard BCR (0.512679 ± 20) to make them consistent with the NIGL measured value for this rock standard (0.512602). Data from the 15°20′ Fracture Zone (Dosso et al., 1991) have been excluded from the shaded field for NA-MORB; dashed line indicates shape of MORB field if these data are included. The 2σ error bar for $^{143}Nd/^{144}Nd$ is based on replicate analyses of J&M Nd standard solution; 2σ error for $^{87}Sr/^{86}Sr$ is within the size of the symbols.

unlikely that a primary Sr-isotope signature can be derived from the material because of the extensive serpentinization. In contrast, an amphibolitized microgabbro from the bottom of Hole 920B has a distinctly lower $^{143}Nd/^{144}Nd$ ratio than Leg 153 gabbros, diabase dikes, or recent on-axis basalts; its Sr-isotope composition is intermediate between that of the massif gabbros and gabbroic dikes from Site 920. One off-axis basalt (Dosso et al., 1993) recovered from just south of Site 922 has a similar isotopic composition to the amphibolitized microgabbro. The only other basalts from the North Atlantic with similar compositions are those from the 15°20′ Fracture Zone (Fig. 3).

Figure 4 summarizes the Pb-isotope variations in the MARK area. In $^{206}Pb/^{204}Pb$ vs. $^{207}Pb/^{204}Pb$ and $^{208}Pb/^{204}Pb$, the data collectively form linear arrays, with all but the peridotites falling within the field of N-MORB. However, similar to Sr-Nd systematics, distinct groups can be identified. The massif gabbros (Sites 921–924) have relatively unradiogenic Pb-isotope compositions that lie at the low end of the N-MORB field, above and parallel to the Northern Hemisphere Reference Line (NHRL). Gabbro dikes from Site 920 overlap the more radiogenic end of the massif gabbro field. The diabase dikes from Site 921 are similar to the massif gabbros in their Pb-isotope composition, but the dikes from Site 920 are significantly more radiogenic. Recent basalts from the neovolcanic zone exhibit a relatively large range of values that extends from the field of massif gabbros to the radiogenic composition of the amphibolite; off-axis basalts (Dosso et al., 1993) show an even larger range. Peridotites from Site 920 lie above the field of MORB at higher $^{207}Pb/^{204}Pb$ and $^{208}Pb/^{204}Pb$ values for a given $^{206}Pb/^{204}Pb$. This has been attributed to alteration-serpentinization processes involving seawater ± pelagic sediments (Kempton and Stephens, this volume).

Because the Leg 153 diabase dikes range from 10% to 50% altered, leaching experiments were conducted to obtain primary isotope values by removing as much of the effects of alteration as possible. In the first leaching experiment, 6M HCl was added to the sample powder, sealed in a Savillex® beaker and placed on a hot plate at ~100°C for 30 min. The resulting Nd-isotope analyses show no systematic differences in composition between leached and unleached powders outside of analytical uncertainty (Table 2). In contrast, leachates have consistently higher Pb-isotope values than leached residues, lying outside the field of MORB and overlapping the field of serpentinized peridotites in some cases (Fig. 4). By analogy with the Site 920 peridotites, this suggests alteration involving seawater ± pelagic sediments.

Sr isotopes also show significant differences (Fig. 5A) between leached residues and leachates. For Site 921 dikes, the leachates have slightly higher $^{87}Sr/^{86}Sr$ values, but residues and unleached powders are either indistinguishable, or the residues are slightly less radiogen-

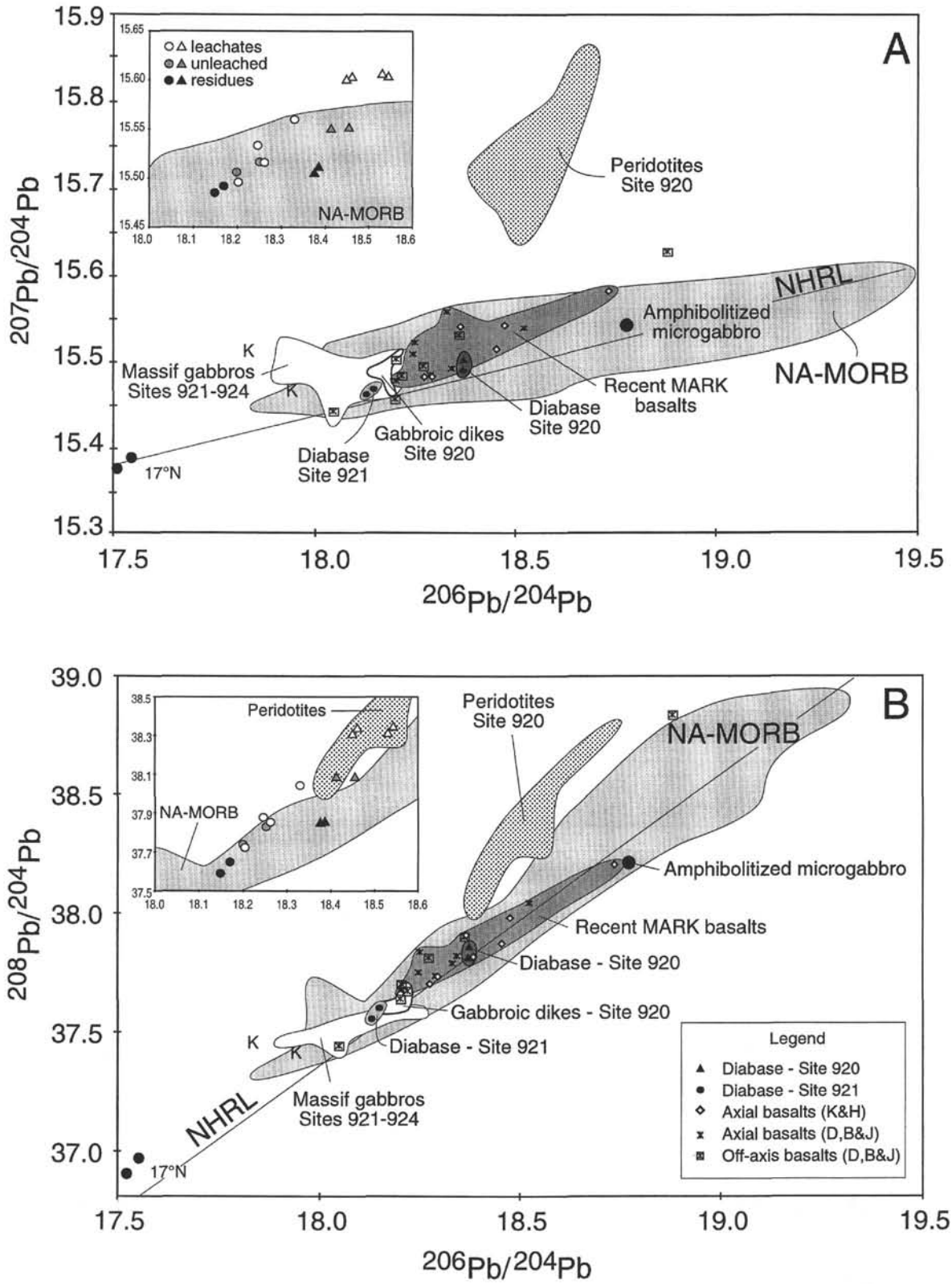

Figure 4. Plot of $^{206}Pb/^{204}Pb$ vs. **(A)** $^{207}Pb/^{204}Pb$ and **(B)** $^{208}Pb/^{204}Pb$; data plotted are average values of leached residues from Table 2. Data for NA-MORB field are from Dupré and Allègre (1980), Dupré et al. (1981), Hamelin et al. (1984), Sun (1980), and sources listed in Figure 3. The unradiogenic end of the NA-MORB field is defined by two samples (K) from the Kane Fracture Zone (Hamelin et al., 1984), and two samples from 17°N (Dosso et al., 1993); these are indicated separately from the main field. Data for off-axis basalts are from Dosso et al. (1993). The field for gabbros from Sites 921 to 924 includes all samples analyzed by Kempton and Hunter (this volume), but note that most fall within a very restricted range of values ($^{206}Pb/^{204}Pb$ = 18.0–18.2). Insets show Pb-isotope results of leaching experiments on diabase dikes from Sites 920 (triangles) and 921 (circles).

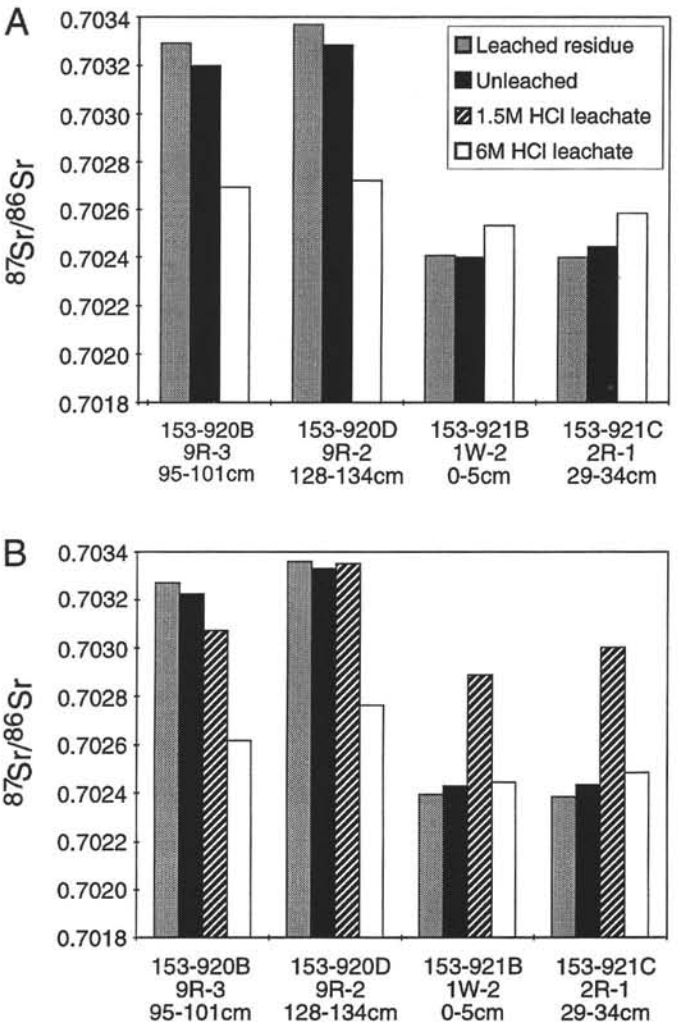

Figure 5. Histogram of Sr-isotope compositions of unleached powders, leached residues, and leachates for diabase dikes from Sites 920 and 921. **A.** Results from the first leaching experiment using only 6-M HCl. **B.** Results of the two-stage leaching experiment involving 1.5-M HCl followed by 6-M HCl. See text for discussion.

ic than the unleached powder. Such results are common and typically attributed to low-temperature alteration involving seawater. In contrast, the leachates from dikes from Site 920 are significantly less radiogenic than either the unleached powders or the leached residues; the unleached powders are intermediate in composition between leachates and residues. This result is unexpected and difficult to explain, particularly when one considers that these dikes are in contact with serpentinized peridotite whose $^{87}Sr/^{86}Sr$ composition is ~0.708–0.709 (Kempton and Stephens, this volume). Therefore, a second leaching experiment was designed in which a first-stage leach of hot 1.5-M HCl was added to the powder for 30 min, followed by a stronger leach in hot 6-M HCl for an additional 30 min, in order to see whether this unradiogenic component was in easily leachable phases such as calcium carbonate or zeolites. The results of this experiment are shown in Figure 5B. The weak HCl leach has a Sr-isotope composition similar to the unleached diabase samples from Site 920, but it has higher $^{87}Sr/^{86}Sr$ than the diabase from Site 921. Again, the strong HCl leach has a less radiogenic composition than the residue of the diabase from Site 920. The significance of these results will be discussed in a subsequent section along with other effects of alteration.

Diabase dikes from Sites 920 and 921 are homogeneously depleted in $\delta^{18}O$ (~ +4.9‰ to +5.2‰) relative to MORB (~+5.7‰). These values (Table 2) are significantly lower than those for clinopyroxene and plagioclase mineral separates from most Leg 153 gabbros (Kempton and Hunter, this volume), but they are typical of the O-isotope compositions of sheeted dikes from Hole 504B (Friedrichsen, 1985).

DISCUSSION

Dikes from Site 920—Primary Magmas, Parental Magmas, or Alteration?

Relative to previously reported chemical compositions (Dosso et al., 1993; Bryan et al. 1994; Reynolds, 1995), diabase dikes from Site 920 have the most MgO-rich basaltic compositions documented thus far from the MARK region (Fig. 1). They also have among the lowest concentrations of incompatible trace elements (Fig. 2). If these compositions are original, they have profound implications for the long-standing debate on the composition of MORB primary magmas (Presnall and Hoover, 1984; Elthon, 1986; Kinzler and Grove, 1992; Falloon and Green, 1988; Jacques and Green, 1980; Fujii and Scarfe, 1985). (Usage of the terms primary, parental, and primitive in this paper follows the definitions recommended by Hess, 1992.) It is generally accepted that most MORBs (MgO < 8 wt%) have experienced crystal fractionation at low pressures, but there is less agreement about the origin of more magnesian MORBs (MgO > 9.5 wt%). Two alternatives have been proposed. They either represent primary magmas containing 10–12 wt% MgO that formed or last equilibrated at pressures of ~10 kbar (Takahashi and Kushiro, 1983; Presnall and Hoover, 1984; Fujii and Scarfe, 1985; Fujii, 1989), or they are the

fractionated products of picritic magmas (15–17 wt% MgO) that were formed at higher pressures of 15–30 kbar (O'Hara, 1968; Stolper, 1980; Falloon and Green, 1987; Elthon, 1989). More recently, Klein and Langmuir (1987) have suggested that partial melting is polybaric, occurring within upwelling oceanic mantle over an interval of about 200°C. Thus a spectrum of primary MORB magma compositions is generated during the partial melting process. The compositions of primary melts generated during this continuous, "pooled" melting process are substantially different from equilibrium batch partial melts.

However, the Site 920 diabase is heavily altered, containing more than 5.5 wt% H_2O, and it is not immediately apparent which chemical characteristics are primary and which are secondary. The diabase from Holes 920B and 920D are believed to be from the same dike (Shipboard Scientific Party, 1995), yet MgO contents vary from 12.14 to 15.08 wt%. In fact, samples taken just 20 cm apart in Hole 920D differ by more than 1 wt% in MgO, Al_2O_3, and CaO (Table 1; Fig. 1). If these compositional differences are original features, it would require either significant local phenocryst accumulation (or loss) or multiple injections of different melt compositions within the same dike, yet there is no evidence for either of these alternatives. Assimilation of altered peridotite (high MgO, but high $^{87}Sr/^{86}Sr$) or gabbro (low $^{87}Sr/^{86}Sr$, but low MgO) during dike emplacement fails to simultaneously account for the relatively constant trace-element concentrations (Fig. 2), Sr-isotope systematics (Fig. 5), and high MgO contents (Fig. 1).

We previously showed (Fig. 1) that diabase from Site 920 is compositionally distinct from recent on-axis basalts. In particular, the analyzed samples display linear trends on oxide-oxide plots that are oblique to the trends of recent MARK basalts; they have higher MgO contents, but lower CaO, FeO, and TiO_2. For illustrative purposes, the MgO vs. CaO diagram is reproduced in Figure 6. Plotted for reference are generalized compositions of primary and secondary phases present in these rocks, as well as the compositions of pooled melts (i.e., instantaneous melts integrated over the melting column) generated by intersection of the solidus at different pressures (Klein and Langmuir, 1987). This figure typifies the major-element systematics. The strong negative correlation between MgO and CaO for the Site 920 dikes is completely at odds with the low positive slope of the recent MARK basalt trend produced by cotectic crystallization of olivine and plagioclase ± clinopyroxene. It is similarly at odds with the curve defined by the change in calculated pooled melt compositions, indicating that compositional differences between the Site 920 diabase samples are not related to partial melting processes. At low pressures, magmas with greater than about 10 wt% MgO will almost certainly have olivine as the only liquidus phase (Francis, 1995). However, the trend shown in Figure 6 is clearly not an olivine control line, as it projects toward a CaO-free composition of about 20–25 wt% MgO, which is more typical of chlorite than olivine (~50 wt% MgO).

Studies of hydrothermally altered basalts have shown that Mg^{2+} is highly reactive during basalt/seawater reactions between 70° and 425° C. Fluids are quickly depleted in Mg^{2+} by the formation of clay minerals, which fix Mg^{2+} in the altered rocks (Bischoff and Dickson, 1975; Seyfried and Mottl, 1982). In particular, in rocks where chlorite and albite are the predominant alteration phases, strong negative correlations between CaO and MgO are observed, whereas those dominated by amphibole and albite show only poor correlations between these elements (Miyashiro et al., 1971; Humphris and Thompson, 1978; Gillis and Thompson, 1993). Thus, replacement of plagioclase by albite and interstitial glass by chlorite leads to a loss in CaO, a gain in Na_2O, and enrichment in MgO. Petrographic descriptions and recent electron microprobe analyses (P.D. Kempton, unpubl. data) of the Site 920 diabase indicate that chlorite and Na-rich plagioclase (An_{14}) are the principal secondary minerals present. However, most of the altered samples in previous studies had MgO contents <12 wt%; those few samples with MgO contents >12 wt% were typically more than 80% altered. In contrast, alteration of the Site 920 diabase is limited to 25%–50%, yet MgO contents reach 15 wt%. This may in part be attributable to differences in occurrence. The Site 920 diabase occurs as a dike crosscutting Mg-rich harzburgite, whereas previous studies focused on the alteration of basalts occurring in a basaltic pile.

Similarly difficult to explain is the strong, and amazingly uniform, enrichment in Sr observed in the Site 920 diabase (Fig. 2). The behavior of Sr during alteration is known to be variable. Humphris and Thompson (1978) observed that Sr and CaO were positively correlated in altered pillow basalts, and they inferred that Sr was leached from the rock during alteration. In contrast, Gillis and Thompson (1993) found no correlation between CaO and Sr in their study of hydrothermally altered basalts from the MARK area; they did, however, observe that Sr and Na_2O were positively correlated, at least for samples where chlorite and albite dominated the alteration assemblage. This is consistent with experimental studies on the partitioning of Sr between plagioclase and hydrothermal fluids that indicate that Sr may be enriched in albite relative to more calcic plagioclase precursors (Blundy and Wood, 1991). Limited Sr data for hydrothermal

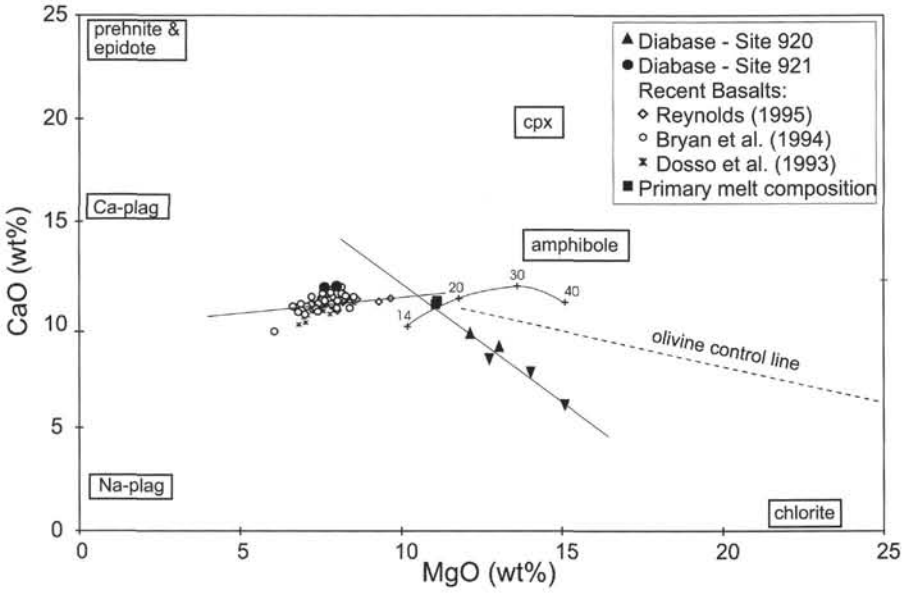

Figure 6. Plot of CaO vs. MgO wt% for diabase dikes from Leg 153 and recent on-axis basalts from MARK (Reynolds, 1995; Bryan et al., 1994; Dosso et al., 1993). Shown for comparison is the curve for "pooled" melt compositions as a result of intersection of the solidus at different pressures; the curve is extrapolated from data points indicated for 14, 20, 30, and 40 kbar from Klein and Langmuir (1987). Shown for comparison are generalized compositions of the main primary and secondary minerals (except olivine) present in these rocks; olivine plots outside of the diagram at MgO contents of ~50 wt%. The primary melt compositions of Sullivan (1991) are plotted as the solid squares.

chlorite suggest that this phase may also act as a sink for Sr (Gillis et al., 1992). Thus, given that chlorite and oligoclase are the most abundant secondary minerals in Site 920 diabase, we attribute the substantial enrichment in Sr (Fig. 2) to the replacement of plagioclase, glass, and other groundmass phases during hydrothermal alteration by chlorite and Na-plagioclase.

However, in spite of the large enrichment in Sr concentration in Site 920 diabase, the Sr-isotope composition of the dikes is not exceedingly high (0.7035); its value still lies within the field of MORB basalts (Fig. 3). That is not to say that these compositions are primary, particularly when considered relative to unaltered gabbros and basalts (~0.70236) from the same area (Kempton and Hunter, this volume). However, they certainly do not reflect extensive interaction with seawater Sr ($^{87}Sr/^{86}Sr = 0.709$) as do the surrounding peridotites (~0.708). Gillis and Thompson (1993) observed that bulk rock $^{87}Sr/^{86}Sr$ ratios were influenced neither by degree of alteration nor by alteration assemblage. Instead, Sr-isotope ratios tended to reflect the degree of albitization of plagioclase and the Sr-isotopic composition of the altering fluid. Clearly, for the Site 920 dikes, where the concentration of Sr has increased by nearly a factor of three, the Sr-isotope composition of the dikes will be dominated by the $^{87}Sr/^{86}Sr$ of the secondary component. This requires that the fluids responsible for alteration of the diabase dikes had a relatively low $^{87}Sr/^{86}Sr$ compared with seawater.

In conjunction with O-isotope data, the Sr-isotope results also suggest that the Site 920 dikes were injected prior to serpentinization, and thus record part of the alteration history of the peridotite massif. At high temperatures (>300°C) of exchange with seawater ($\delta^{18}O = 0$), the $\delta^{18}O$ of a magmatic plagioclase (~+5.9‰) will decrease; at lower temperatures, the $\delta^{18}O$ will increase because of this same interaction. How much the $\delta^{18}O$ increases or decreases depends on the seawater/rock ratio (W/R) and the relative resistance of phases to O-isotope exchange. For example, pyroxene (whose $\delta^{18}O_{magmatic} = +5.4‰$) is more resistant to oxygen-isotope exchange with fluids than plagioclase. The depletion in ^{18}O seen in dikes, both from Site 920 and Site 921, indicates interaction with seawater at moderate temperatures (250°–300°C) where the $\Delta_{rock\text{-}water}$ values are about +5.0‰.

The mineralogical controls on Sr partitioning discussed above also indicate that Sr-isotope exchange is at least indirectly dependent on temperature (Berndt et al., 1988). We know that mixed-layer smectite/chlorite first appears at temperatures from 150° to 180°C and discrete chlorite appears at temperatures between 230° and 275°C (Schiffman and Fridleifsson, 1991). Actinolite stability is estimated at ~250°C to >300°C (Bird et al., 1984), and at >400°C more aluminous amphiboles are present (Gillis and Thompson, 1993). The absence of aluminous amphibole, but presence of actinolite (P.D. Kempton, unpubl. data), argues for alteration of the Site 920 diabase at temperatures <400°C, but probably >250°C. These temperatures of alteration are broadly consistent with those calculated for serpentinization of the surrounding peridotite column (>350°C) on the basis of O-isotope fractionation between serpentine and magnetite (Agrinier and Cannat, this volume). However, Agrinier and Cannat (this volume) argue that the consistently low $\delta^{18}O$ values (+2.5 to +4.1‰) they obtained for the Site 920 peridotites indicate that all of the ultramafic rocks recovered from this site were serpentinized during a single, rapid, pervasive high-temperature event.

Given that the peridotites have uniformly high $^{87}Sr/^{86}Sr$ ratios (Kempton and Stephens, this volume), this conclusion is in apparent conflict with the results from the crosscutting diabase dikes because it suggests that the high-temperature hydrothermal fluids also had high $^{87}Sr/^{86}Sr$. This is difficult to reconcile with the consistently low Sr-isotope compositions of the dikes. In trying to resolve this paradox, several observations must be accounted for simultaneously: (1) the diabase dikes have low $^{87}Sr/^{86}Sr$, but are significantly enriched in Sr, (2) the secondary mineral assemblage, as well as O-isotope data, suggest that alteration of the Site 920 diabase occurred at moderate temperatures (~250–300°C), (3) Site 920 peridotites have high $^{87}Sr/^{86}Sr$, but low Sr concentrations, and (4) O isotopes suggest that serpentinization of the Site 920 peridotites occurred over a limited range of high temperatures (Agrinier and Cannat, this volume).

Gillis and Thompson (1993) have argued that episodic magmatic and hydrothermal events at slow-spreading ridges result in mineral assemblages that are the cumulative effects of more than one hydrothermal event as crustal segments migrate off axis. If we assume that alteration of the dikes occurred at high temperatures, at the same time as serpentinization of the peridotite, and that the hydrothermal fluids involved had a high $^{87}Sr/^{86}Sr$ signature, subsequently restoring the dikes to a less radiogenic, more MORB-like value would be difficult: (a) because of the high Sr concentrations of the dikes relative to hydrothermal fluids, and (b) because there is no obvious source of fluids having low $^{87}Sr/^{86}Sr$. Magmatic fluids are simply of insufficient volume. Hydrothermal fluids venting from hot springs in the MARK area have an appropriately low $^{87}Sr/^{86}Sr$ composition of ~0.7028 (Campbell et al., 1988), but even if such fluids were subsequently available to alter the dikes, given the significantly lower Sr concentration of the peridotite relative to the diabase, one would expect to find portions of the peridotite column affected as well; yet the peridotite appears to be relatively homogeneous in O- and Sr-isotope composition.

Therefore, we propose that the Sr-isotope composition of the diabase is indicative of the fluids during the earliest stages of alteration of the peridotite section. O-isotope compositions require that these fluids were originally derived from seawater, but their Sr-isotope compositions could initially have been buffered to lower $^{87}Sr/^{86}Sr$ values by interaction with a basalt/gabbro carapace overlying the peridotite at the time of alteration. With uplift, both peridotites and dikes would become exposed to fluids having more radiogenic (i.e., seawater-like) Sr-isotope signatures. Although low-temperature fluid interaction is not recorded in the O-isotope signatures of the four serpentinites analyzed from Site 920 (Agrinier and Cannat, this volume), Hébert et al. (1990) analyzed nine serpentinized peridotites from Site 670 (located ~20 km south) and reported predominantly high $\delta^{18}O$ values (up to +8.8‰). Their results yield temperatures of serpentinization of 110° to 385°C, confirming at least local reequilibration to lower temperatures. Because the concentration of Sr in the peridotites (~3 ppm; Stephens, this volume) is lower than in seawater (~8 ppm; Faure, 1986), Sr isotopes could be altered during low-temperature reequilibration/alteration even if O isotopes remain unaffected. The low $^{87}Sr/^{86}Sr$ ratios of the dikes would not be overprinted by these processes (1) because of the higher Sr contents of the dikes relative to the hydrothermal fluids, and (2) because chlorite, the principal alteration phase in the diabase, is stable and does not exchange readily by diffusion at the temperatures of serpentinization (<400°C). The origin of the low $^{87}Sr/^{86}Sr$ ratios (0.7027) of the 6-M HCl leachates is enigmatic (Fig. 5). A complete understanding of these results will require more detailed Sr- and O-isotopic analyses and identification of the minerals in which the different Sr-isotope components reside.

Although the data discussed above provide ample evidence for modification of the chemical and isotopic compositions of the Site 920 diabase during hydrothermal alteration, the rocks, nevertheless, have Ni and Cr contents (Table 1) that cannot be accounted for through alteration processes (Humphris and Thompson, 1978; Gillis and Thompson, 1993). These concentrations are higher than both recent MARK basalts and Site 921 diabase dikes by a factor of 2.5. This indicates that the Site 920 diabase is more primitive than recent on-axis basalts. Figure 7, a plot of Ni vs. Zr, shows a trend for recent MARK basalts that is consistent with fractionation of olivine + plagioclase ± clinopyroxene. The Site 921 dikes lie within this field. However, the trend shown by the Site 920 dikes has a significantly steeper slope at lower Zr and higher Ni contents and suggests fractionation (or accumulation) of olivine alone. If we assume that the Ni

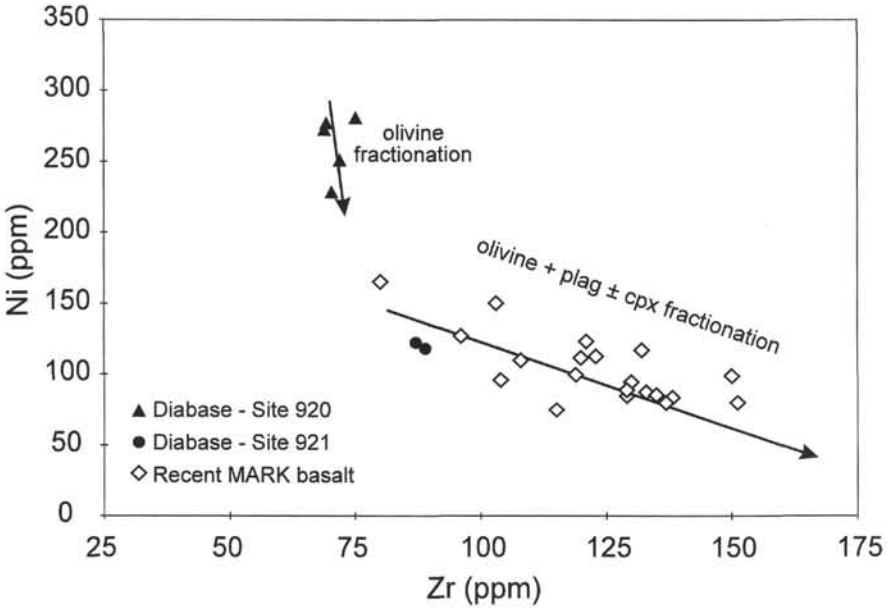

Figure 7. Plot of Zr vs. Ni (in ppm) for diabase dikes from Sites 920 and 921. Data for recent axial basalts from Reynolds (1995). The lines shown are only to highlight the variations observed and are not calculated trace-element fractionation trends.

concentrations in these rocks have not been modified by significant fractionation of olivine prior to crystallization, they are consistent with mantle melts containing 10–11 wt% MgO (Klein and Langmuir, 1987).

We can also estimate the original composition of the diabase if we assume that the intersection point of the two trends in MgO vs. oxides (Fig. 1) is indicative of the diabase composition prior to alteration (Fig. 6). Using CaO, TiO_2, and FeO vs. MgO, this method estimates the MgO contents of the original diabase at between 10 and 11 wt%, consistent with the qualitative estimate based on the Ni contents. Note that slightly higher MgO contents would be estimated if the fractionation history includes an early stage consisting of olivine only. The trends also intersect at significantly higher MgO contents (~12.5 wt%) if SiO_2 and Al_2O_3 are used. However, this latter estimate is probably in error, and reflects the less systematic behavior of SiO_2 and Al_2O_3 during alteration (Fig. 1; Humphris and Thompson, 1978; Gillis et al., 1993). Conversely, we can use the calculated MgO contents to infer the original oxide concentrations. These calculations yield approximately 11.5 wt% CaO, 7.7 wt% FeO, 2.3 wt% Na_2O, and 0.8 wt% TiO_2. These concentrations are similar to the primitive melt compositions calculated on the basis of melt inclusions in plagioclase and olivine from the MARK area (Sullivan, 1991). Concentrations of SiO_2 (47.8 wt%) and Al_2O_3 (18.0 wt%) are lower and higher, respectively, than the Sullivan (1991) primary melt compositions, but again these estimates probably reflect alteration effects because SiO_2 and Al_2O_3 are not as well correlated with MgO as the other major elements. Clearly, these estimates are dependent on the assumption that the original composition lies on an extension of the trend defined by the recent MARK basalts. If the older lavas in the MARK area had higher Ca and Al and lower Ti and Fe, as suggested by the Site 921 diabase dikes (Fig. 1), the intersection of the two trends would occur at lower MgO contents (~9.5 wt%). Thus, although the extremely high MgO contents of the Site 920 diabase samples are clearly the product of alteration processes, the data—after alteration effects are removed—are consistent with a composition that is among the most primitive reported for the MARK area. In this context, the occurrence of the dikes in the peridotite section may be more than fortuitous—it may be evidence that these magmas avoided the significant modifying effects of magma mixing and fractional crystallization in a magma chamber. If so, the major- and trace-element composition of the Site 920 diabase (before alteration) may be typical of some of the primitive/parental melts injected into the magma plumbing system at MARK.

Speculations on Depth of Melting, Degree of Melting, and Source Variations with Time

Much work in recent years has gone into understanding the nature of melting in the mantle beneath mid-ocean ridges. From these studies, we now know that this process depends not only on the initial mantle composition, but also on the degree of melting, initial depth of melting, depth at which melting terminates, style (i.e., batch vs. fractional), and geometry of melting (Langmuir et al., 1992; Bown and White, 1994; Shen and Forsyth, 1995). We can infer some of these parameters from major-element systematics. For example, Na_2O concentration in a melt is roughly inversely proportional to the extent of melting, whereas FeO tends to increase with increasing pressure of melting. In contrast, Al_2O_3 decreases with increasing pressure (Klein and Langmuir, 1987, and references therein). The behavior of CaO is variable, depending on whether clinopyroxene is residual after melting. However, because low-pressure fractional crystallization affects the major-element compositions of magmas, it is necessary to first correct for these effects. We have done this for the diabase samples from Site 921 by normalizing their compositions to an MgO content of 8 wt% (Langmuir et al., 1992). The calculated Al_8, Ca_8, Na_8, Ti_8, Fe_8, and Ca_8/Al_8 values for diabase from Site 921 are shown in Table 3, along with the range of values calculated for recent axial basalts (data of Reynolds, 1995; Bryan et al., 1994). The normalized concentrations show that the Site 921 dikes have higher Al_8 and Ca_8 than the range of calculated values for recent MARK basalts. Na_8, Ti_8, and Fe_8 values for the diabase fall within the range for recent MARK basalts, but they are restricted to the lower end of the range. Assuming a similar starting source composition, the low Na_8 and Fe_8, combined with the high Al_8, suggest that diabase from Site 921 was generated by a larger degree of melting at shallower depths than most recent basalts from the neovolcanic zone.

Variations in incompatible trace-element ratios are consistent with these qualitative arguments. This is shown diagrammatically in Figure 8, a plot of Zr vs. Y. We have used these two elements because the bulk partition coefficients between crystals and mafic liquids are low for both Zr and Y, and they are not easily fractionated relative to one another during low-pressure crystallization involving only oliv-

Table 3. Calculated oxide concentrations at 8 wt% MgO.

Hole, core, section: Interval (cm):	921B-1W-2 0–5	921C-2R-1 29–34	MARK basalts (range)
Al_8	16.97	17.13	15.19–16.97
Ca_8	11.86	11.94	10.37–11.80
Na_8	2.58	2.61	2.68–3.17
Ti_8	1.38	1.19	1.19–1.77
Fe_8	8.44	8.13	8.25–10.25
Ca_8/Al_8	0.7	0.7	0.67–0.72

ine and plagioclase. However, the partition coefficients for Zr and Y are higher and differ by almost an order of magnitude in clinopyroxene (Hack et al., 1994; Forsythe et al., 1994) so that these two elements can be fractionated during small degrees of partial melting or by fractional crystallization involving sufficient amounts of clinopyroxene. Two observations from this figure are worthy of note:

1. The Leg 153 diabase dikes lie within the field of data shown by Bryan et al. (1994) for the MARK area, but they have among the lowest Zr and Y concentrations. In fact, Bryan et al. (1994) report that most Zr values less than 100 ppm are due to the dilution effect of plagioclase accumulation. Yet, the low Zr and Y contents of diabase from both Sites 920 and 921 cannot be explained in this way because they are not strongly phyric and they are relatively primitive (i.e., MgO ≥ ~8 wt%). We therefore conclude that the low Zr and Y concentrations are an intrinsic characteristic acquired at source. The only rocks in the MARK area with lower Zr and Y concentrations are some high-Al basalts from an older uplifted fault block located between Sites 921 and 920. When compared with the Site 920 diabase, these rocks are not exceptionally MgO rich (8 wt%), although they are considered primitive by Bryan et al. (1994). They cannot, however, be related to the rest of the basalts at MARK by low-pressure fractional crystallization.
2. Diabase from Sites 920 and the older high-Al primitive basalts are similar in their Zr/Y ratios, whereas Site 921 diabase has lower Zr/Y ratios. Recent basalt glasses from the neovolcanic zone (data of Reynolds, 1995) overlap the low values, but trend away from the Site 921 diabase toward both higher Zr/Y ratios and higher concentrations of Zr and Y. Some of this variation is almost certainly due to enrichment during fractional crystallization processes. However, as pointed out earlier, Zr and Y are not easily fractionated relative to one another during low-pressure crystallization involving only olivine and plagioclase. Therefore, for the more primitive compositions, variations in Zr/Y either reflect variations in source composition or partial melting processes (i.e., Zr/Y increases with decreasing degree of partial melting).

The trace-element variations shown in Figure 8 are consistent with smaller degrees of melting for some recent basalts than for diabase from Site 921, in common with the interpretation based on major-element characteristics. In spite of the very low concentrations of Zr and Y in the Site 920 diabase, the higher Zr/Y ratios (Table 1) suggest that they were generated by a smaller degree of partial melting than Site 921 diabase. The low Zr and Y concentrations of the Site 920 diabase are consistent with their primitive composition (i.e., they have experienced little enrichment in incompatible trace elements through fractional crystallization).

Figure 9 quantitatively illustrates these interpretations. Taking depleted MORB mantle similar to that used by Johnson and Dick (1992) as a starting composition, the model calculates "pooled" melt compositions by integrating instantaneous melts over the melting column (Klein and Langmuir, 1987; Langmuir et al., 1992). The results of these calculations indicate that the Site 920 diabase samples are consistent with a pooled melt generated by <15% melting of mantle peridotite in the spinel facies (i.e., shallow depths of melting). Note that calculations involving garnet fail to match the patterns for basalts from the MARK area; this is consistent with the results of Casey (this volume). The critical feature in this model is the enrichment in Zr relative to Nd and Sm, which is diagnostic of relatively low degrees of melting in the spinel facies. This positive Zr anomaly diminishes and eventually disappears at higher degrees of melting (Fig. 9). Langmuir et al. (1992) reported that the variation in Zr/Sm ratio in MORBs is small (~30.6 ± 1.7), yet the Site 920 diabase samples have higher Zr/Sm ratios of 33–36 (Table 1). Most recent MARK basalts are more similar to average MORB, but nonetheless have slightly high Zr/Sm ratios 32.2 ± 1.4 (Reynolds, 1995; Dosso et al., 1993). This is apparent as small Zr anomalies in Figures 2 and 9. In contrast, the Site 921 diabase samples (Zr/Sm = ~30) are indistinguishable from average MORB. Thus, based on these model calculations we suggest that (1) the Site 920 diabase samples are consistent with a pooled melt generated by <15%, but >5%, melting of mantle peridotite in the spinel facies (i.e., shallow depths of melting), (2) recent MARK basalts and Site 921 diabase were generated by slightly larger degrees of melting (>15%) than dikes from Site 920, and (3) the Site 921 diabase falls within the range of recent MARK basalts, but ranks among those generated by the largest degrees of partial melting.

If the results from Site 921 diabase dikes are extrapolated to include the massif gabbros at Sites 921–924, the data suggest that <1 m.y. ago, the degree of melting may have been slightly larger and occurred at shallower depths on average than today in the neovolcanic zone. We acknowledge that this extrapolation may not be justified on the basis of so few diabase samples because we cannot be certain that they are representative of the magmatism at the time. However, isotopic data provide strong evidence for temporal changes in the composition of the mantle source in the MARK area over this period.

Considered collectively, gabbros, diabase dikes, and recent basalts from MARK demonstrate a relatively large range in primary isotope compositions within a relatively small geographic area (Figs. 3, 4). Within that range, gabbros and dikes from Site 921 exhibit only limited variations in Sr-, Nd-, and Pb-isotope characteristics, but recent basalts (Kempton and Hunter, this volume) have significantly lower Nd- and higher Pb-isotope compositions, and there is almost no overlap between the two. Data from Dosso et al. (1993) suggest a greater overlap in Nd-isotope composition between the massif gabbros and the recent basalts, but this data set includes no information on standard values, so correcting for interlaboratory bias was not possible. Given the small differences involved, and the size of the analytical uncertainty for Nd isotopes (see Fig. 3), we prefer to base our analysis on data acquired in our own laboratory so that all isotopic data are internally consistent. The Nd-isotope data of Dosso et al. (1993) will therefore be excluded from our discussion. Although Sr- and Pb-isotope characteristics have been modified during serpentinization of the peridotites, Nd isotopes are unaffected, and demonstrate that ultramafic rocks from Site 920 have the highest Nd-isotope ratios in the MARK area.

Because all of the rocks considered here are relatively young (<0.75 m.y. old), differences in Nd- and Sr-isotope compositions between the recent basalts and the more depleted massif gabbros and Site 921 diabase dikes cannot be the result of radioactive decay; nor are they the product of secondary alteration processes (Kempton and Hunter, this volume). Therefore, in order to produce the variations shown in Figures 3 and 4, the recent on-axis basalts must have been derived from an isotopically distinct magmatic source compared with that for the gabbros and Site 921 diabase dikes, which are older. This is particularly apparent from the Pb-isotope systematics, where the recent MARK basalts show no overlap at all with the older gabbros and diabase dikes from Site 921 (Fig. 4). Taken collectively, there is clearly a gradual shift in composition from the most depleted among North Atlantic MORB (i.e., Site 920 peridotites, massif gabbros, and Site 921 diabase) to less depleted (recent axial basalts).

In this scenario, the relative importance of rare compositions like the Site 920 diabase or the amphibolitized microgabbro is unclear.

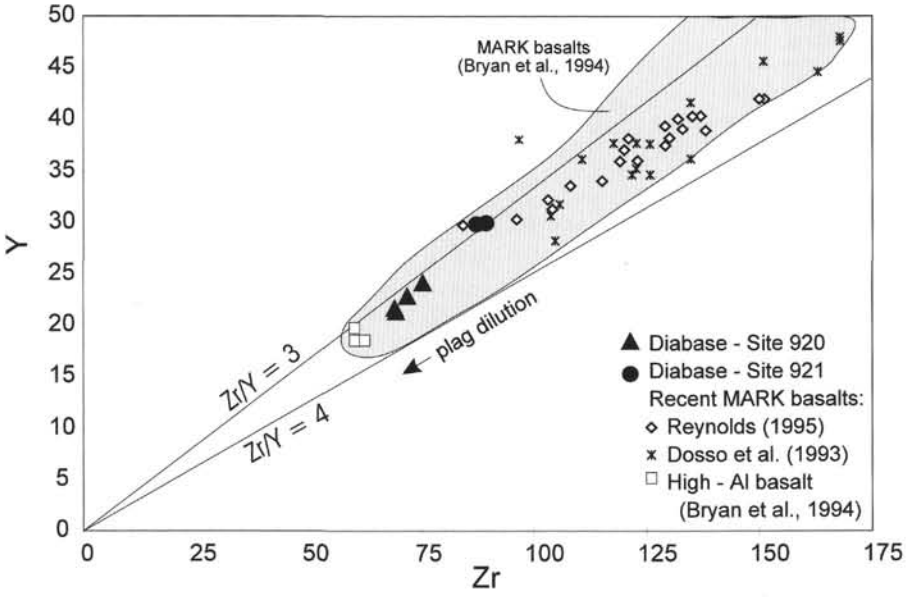

Figure 8. Plot of Zr vs. Y concentrations (in ppm) for Leg 153 diabase dikes compared with recent MARK basalts (Bryan et al.,1994; Reynolds, 1995; Dosso et al., 1993).

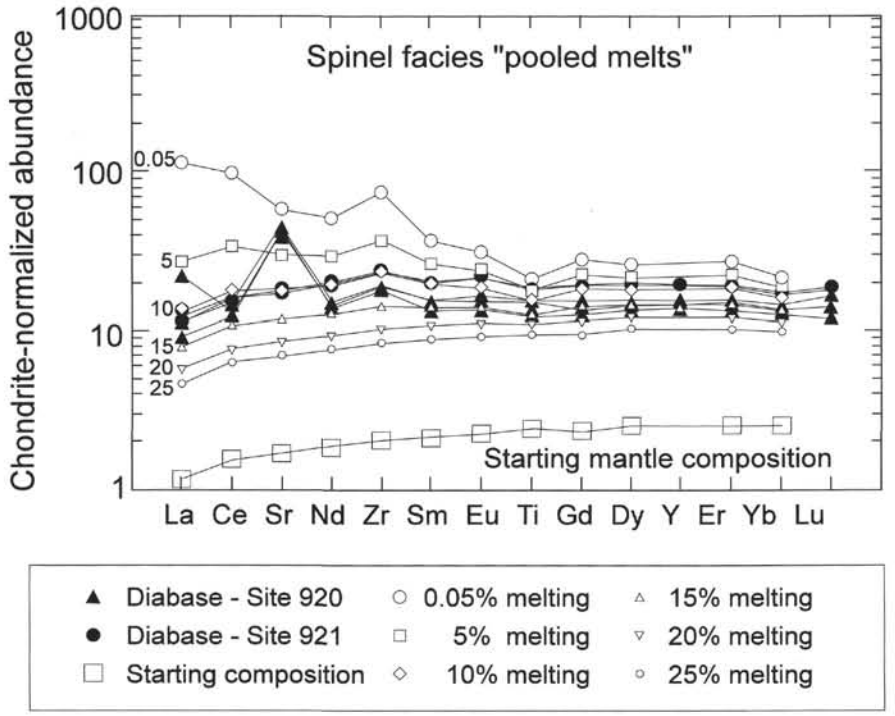

Figure 9. Model compositions of pooled melts shown in a chondrite-normalized trace-element plot. Starting mantle composition as in Johnson and Dick (1992); partition coefficients are given in Casey (this volume). The synthetic melts in the diagram show 0.05%, 5%, 10%, 15%, 20%, and 25% melting and pooled melt compositions produced via a near-fractional melting model with 1% residual porosity. See text for discussion.

These rocks are isotopically unique relative to other basaltic and gabbroic rocks from MARK (Figs. 3, 4) and apparently at odds with a model involving a gradual shift in isotopic composition of a homogeneous mantle source with time. It might be argued that the spectrum of isotopic compositions observed at MARK is the product of mixing between depleted and enriched (or at least less depleted) mantle components, with the peridotites and/or massif gabbros representative of the more-depleted end member and the Site 920 diabase and amphibolitized microgabbro representative of the less-depleted end member. The lower Nd-isotope ratios and flatter REE patterns of the Site 920 diabase relative to other MARK basalts and gabbros are consistent with this interpretation. However, binary mixing between the Site 920 diabase and a more-depleted component cannot explain the whole range of chemical and isotopic characteristics observed in the samples studied. In particular, some recent basalts have significantly more radiogenic Pb-isotope ratios than the Site 920 diabase. The amphibolitized microgabbro has sufficiently low $^{143}Nd/^{144}Nd$ and high Pb-isotope ratios (Fig. 4) that it could be representative of the less-depleted end member isotopically, but the major- and trace-element characteristics of its parental magma are unknown. Nevertheless, whether or not these particular examples of less-depleted mantle compositions are representative, their contemporaneity with rocks derived from more-depleted sources supports a mixing model in which the proportion of enriched to depleted mantle components changes with time, rather than a gradual compositional shift of a homogeneous source.

The restriction of unusual compositions like the Site 920 diabase and amphibolitized microgabbro to the peridotite section, which is itself located near the accommodation zone, may be significant. The paucity of lower crustal rocks in the nontransform offset indicates

that the crust in this region is unusually thin. Study of ridge segments to the north of MARK (MARNOK) have demonstrated that small volumes of unusual, enriched compositions are more likely to remain distinct and erupt at the edges of spreading cells where magma supply rates are lower. Toward the middle of spreading cells, enriched compositions become incorporated into existing magma chamber(s) and are homogenized. It may mean that these relatively unusual compositions are preserved only in areas where magmatism is low.

CONCLUSIONS

1. Diabase dikes from Site 920 represent some of the most primitive magmas yet recovered from the MARK area. Concentrations of most major elements and some trace elements (e.g., Sr) have been strongly modified by hydrothermal alteration, but linear relationships on oxide-oxide plots make it possible to reconstruct their original compositions. These calculations indicate that, before alteration, the diabase contained about 11 wt% MgO and was remarkably similar to the primary melt compositions for the MARK area proposed by Sullivan (1991). This estimate is consistent with the high Ni and Cr contents and low concentrations of incompatible trace elements in the diabase. Lower $^{143}Nd/^{144}Nd$ ratios and flatter REE patterns are consistent with a less-depleted source for the Site 920 diabase than that giving rise to the majority of MARK basalts.
2. Sr-isotope data indicate that the fluids responsible for alteration of the Site 920 diabase had a relatively low $^{87}Sr/^{86}Sr$ (~0.703) compared with seawater (0.709), yet the depletion in ^{18}O seen in Leg 153 dikes (+4.9‰ to +5.2‰) indicates interaction with seawater at moderate temperatures (250°–300°C). These data, combined with mineralogical constraints, indicate that injection of the Site 920 diabase into the peridotites must have occurred before serpentinization, but that the Sr-isotope compositions of the fluids involved were buffered to lower values by interaction with an overlying basalt/gabbro carapace. Low-temperature interaction between seawater and the uplifted peridotite massif did not overprint the low Sr-isotope signatures of diabase as it did the peridotites because (a) the Sr concentration of the diabase is very high (~300 ppm), and (b) chlorite, the principal secondary mineral present, does not exchange readily by diffusion at the temperatures of serpentinization.
3. Major-element and trace-element modeling demonstrate that (a) the Site 920 diabase samples are consistent with a pooled melt generated by <15% melting of mantle peridotite in the spinel facies (i.e., shallow depths of melting), and (b) recent MARK basalts and diabase from Site 921 were generated by slightly larger degrees of melting (>15 wt%) than dikes from Site 920.
4. The average isotopic composition within the MARK area has changed over a period of <1 m.y., becoming more radiogenic in Pb, but less radiogenic in Nd-isotope composition with time, indicating that the source is currently more enriched on average than that available ~750,000 yr earlier. However, the contemporaneity of rocks derived from relatively depleted sources (i.e., Sites 921–924 gabbros and Site 921 dikes) and those from significantly less depleted sources (i.e., Site 920 diabase and amphibolitized microgabbro) supports a mixing model in which the proportion of enriched to depleted mantle components changes with time, rather than a gradual compositional shift of a homogeneous source.
5. Restriction/preservation of distinctive compositions (e.g., the Site 920 diabase and amphibolitized microgabbro) to the peridotite sections at Site 920 may be due to the lower magma supply rates expected near the boundary of a spreading cell.

ACKNOWLEDGMENTS

We would like to thank Pat Castillo, Jennifer Reynolds, and an anonymous reviewer for constructive reviews; their input greatly improved the paper. Support for this work was provided by NERC grant GST/02/990. This paper represents NIGL Publication Series #160.

REFERENCES

Berndt, M.E., Seyfried, W.E., and Beck, J.W., 1988. Hydrothermal alteration processes at mid-ocean ridges: experimental and theoretical constraints from Ca and Sr exchange reactions and Sr isotopic ratios. *J. Geophys. Res.*, 93:4573–4583.

Bird, D.K., Schiffman, P., Elders, W.A., Williams, A.E., and McDowell, D., 1984. Calc-silicate mineralization in active geothermal systems. *Econ. Geol.*, 79:671–695.

Bischoff, J.L., and Dickson, F.W., 1975. Seawater-basalt interaction at 200°C and 500 bars: implications for origin of seafloor heavy metal deposits and regulation of seawater chemistry. *Earth Planet. Sci. Lett.*, 25:385–397.

Blundy, J.D., and Wood, B.J., 1991. Crystal-chemical controls on the partitioning of Sr and Ba between plagioclase feldspar, silicate melts and hydrothermal solutions. *Geochim. Cosmochim. Acta,* 55:193–209.

Bown, J.W., and White, R.S., 1994. Variation with spreading rate of oceanic crustal thickness and geochemistry. *Earth Planet. Sci. Lett.,* 121:435–449.

Bryan, W.B., Humphris, S.E., Thompson, G., and Casey, J.F., 1994. Comparative volcanology of small axial eruptive centers in the MARK area. *J. Geophys. Res.,* 99:2973–2984.

Bryan, W.B., Thompson, G., and Ludden, J.N., 1981. Compositional variation in normal MORB from 22°–25°N: Mid-Atlantic Ridge and Kane Fracture Zone. *J. Geophys. Res.*, 86:11815–11836.

Campbell, A.C., Palmer, M.R., Klinkhammer, G.P., Bowers, T.S., Edmond, J.M., Lawrence, J.R., Casey, J.F., Thompson, G., Humphris, S., Rona, P.A., and Karson, J.A., 1988. Chemistry of hot springs on the Mid-Atlantic Ridge. *Nature,* 335:514–519.

Cannat, M., Karson, J.A., Miller, D.J., et al., 1995. *Proc. ODP, Init. Repts.,* 153: College Station, TX (Ocean Drilling Program).

Cohen, R.S., Evensen, N.M., Hamilton, P.J., and O'Nions, R.K., 1980. U-Pb, Sm-Nd, and Rb-Sr systematics of mid-ocean ridge basalt glasses. *Nature,* 283:149–153.

Cohen, R.S., and O'Nions, R.K., 1982. The lead, neodymium and strontium isotopic structure of ocean ridge basalts. *J. Petrol.,* 23:299–324.

Craig, H., 1961. Standard for reporting concentrations of deuterium and oxygen-18 in natural waters. *Science,* 133:1833–1834.

Dosso, L., Bougault, H., and Joron, J.L., 1993. Geochemical morphology of the North Atlantic Ridge, 10°–24°N: trace element-isotope complementarity. *Earth Planet. Sci. Lett.,* 120:443–462.

Dosso, L., Hanan, B.B., Bougault, H., Schilling, J.G., and Joron, J.L., 1991. Sr-Nd-Pb geochemical morphology between 10 degrees N and 17 degrees N on the Mid-Atlantic Ridge—a new MORB isotope signature. *Earth Planet. Sci. Lett.,* 106:29–43.

Dupré, B., and Allègre, C.J., 1980. Pb-Sr-Nd isotopic correlation and the chemistry of the North Atlantic mantle. *Nature,* 286:17–22.

Dupré, B., Lambret, B., Rousseau, D., and Allègre, C.J., 1981. Limitations of the scale of mantle heterogeneities under ocean ridges. *Nature,* 294:552–554.

Elthon, D., 1986. Comments on "Composition and depth of origin of primary mid-ocean ridge basalts" by D.C. Presnall and J.D. Hoover. *Contrib. Mineral. Petrol.,* 94:253.

————, 1989. Pressure of origin of primary mid-oceanic ridge basalts. *In* Saunders, A.D., and Norry, M.J. (Eds.), *Magmatism in the Ocean Basins.* Geol. Soc. Spec. Publ. London, 42:125–136.

Falloon, T.J., and Green, D.H., 1987. Anhydrous partial melting of MORB pyrolite and other peridotite compositions at 10 kbar: implications for the origin of primitive MORB glasses. *Mineral. Petrol.,* 37:181–219.

————, 1988. Anhydrous partial melting of peridotite from 8 to 35 kbar and the petrogenesis of MORB. *J. Petrol. Spec. Lithosphere Iss.,* 379–414.

Faure, G., 1986. *Principles of Isotope Geology:* New York (Wiley).

Forsythe, L.M., Nielsen, R.L., and Fisk, M.R., 1994. High-field-strength element partitioning between pyroxene and basaltic to dacitic magmas. *Chem. Geol.,* 117:107–125.

Francis, D., 1995. The implications of picritic lavas for the mantle sources of terrestrial volcanism. *Lithos,* 34:89–105.

Frey, F.A., Walker, N., Stakes, D., Hart, S.R., and Nielsen, R., 1993. Geochemical characteristics of basaltic glasses from the AMAR and FAMOUS axial valleys, Mid-Atlantic Ridge (36°–37°N): petrogenetic implications. *Earth Planet. Sci. Lett.,* 115:117–136.

Friedrichsen, H., 1985. Strontium, oxygen, and hydrogen isotope studies on primary and secondary minerals in basalts from the Costa Rica Rift, Deep Sea Drilling Project Hole 504B, Leg 83. *In* Anderson, R.N., Honnorez, J., Becker, K., et al., *Init. Repts. DSDP,* 83: Washington (U.S. Govt. Printing Office), 289–295.

Fujii, T., 1989. Genesis of mid-ocean ridge basalts. *In* Saunders, A.D., and Norry, M.J. (Eds), *Magmatism in the Ocean Basins.* Geol. Soc. Spec. Publ. London, 42:137–146.

Fujii, T., and Scarfe, C.M., 1985. Composition of liquids coexisting with spinel lherzolite at 10 kbar and the genesis of MORBs. *Contrib. Mineral. Petrol.,* 90:18–28.

Gillis, K.M., Ludden, J.N., and Smith, A.D., 1992. Mobilization of REE during crustal aging in the Troodos Ophiolite, Cyprus. *Chem. Geol.,* 98:71–86.

Gillis, K.M., and Thompson, G., 1993. Metabasalts from the Mid-Atlantic Ridge: new insights into hydrothermal systems in slow-spreading crust. *Contrib. Mineral. Petrol.,* 113:502–523.

Hack, P.J., Nielsen, R.L., and Johnston, A.D., 1994. Experimentally determined rare-earth element and Y partitioning behavior between clinopyroxene and basaltic liquids at pressures up to 20 kbar. *Chem. Geol.,* 117:89–105.

Hamelin, B., Dupré, B., and Allègre, C.J., 1984. Lead-strontium isotopic variations along the East Pacific Rise and the Mid-Atlantic Ridge: a comparative study. *Earth Planet. Sci. Lett.,* 67:340–350.

Hébert, R., Adamson, A.C., and Komor, S.C., 1990. Metamorphic petrology of ODP Leg 109, Hole 670A serpentinized peridotites: serpentinization processes at a slow spreading ridge environment. *In* Detrick, R., Honnorez, J., Bryan, W.B., Juteau, T., et al., *Proc. ODP, Sci. Results,* 106/109: College Station, TX (Ocean Drilling Program), 103–115.

Hess, P.C., 1992. Phase equilibria constraints on the origin of ocean floor basalts. *In* Phipps Morgan, J., Blackman, D.K., and Sinton, J.M. (Eds.), *Mantle Flow and Melt Generation at Mid-Ocean Ridges.* Geophys. Monogr., Am. Geophys. Union, 71:67–102.

Humphris, S.E., and Thompson, G., 1978. Trace element mobility during hydrothermal alteration of oceanic basalts. *Geochim. Cosmochim. Acta,* 42:127–136.

Ito, E., White, W.M., and Göpel, C., 1987. The O, Sr, Nd and Pb isotope geochemistry of MORB. *Chem. Geol.,* 62:157–176.

Jacques, A.L., and Green, D.H., 1980. Anhydrous melting of peridotite at 0–15 kbar pressure and the genesis of tholeiitic basalts. *Contrib. Mineral. Petrol.,* 73:287–310.

Johnson, K.T.M., and Dick, H.J.B., 1992. Open system melting and temporal and spatial variation of peridotite and basalt at the Atlantis II fracture zone. *J. Geophys. Res.,* 97:9219–9241.

Karson, J.A., 1991. Accommodation zones and transfer faults: integral components of Mid-Atlantic Ridge extensional systems. *In* Peters, U.J., Nicolas, A., and Coleman, R.G. (Eds.), *Ophiolites Genesis and Evolution of Oceanic Lithosphere:* Dordrecht (Kluwer Academic), 21–37.

Kinzler, R.J., and Grove, T.L., 1992. Primary magmas of mid-ocean ridge basalts, 1. Experiments and methods. *J. Geophys. Res.,* 97:6885–6906.

Klein, E.M., and Langmuir, C.H., 1987. Global correlations of ocean ridge basalt chemistry with axial depth and crustal thickness. *J. Geophys. Res.,* 92:8089–8115.

Langmuir, C.H., Klein, E., and Plank, T., 1992. Petrological systematics of mid-ocean ridge basalts: constraints on melt generation beneath ocean ridges. *In* Morgan, J.P., Blackman, D.K., Sinton, J.M. (Eds.), *Mantle Flow and Melt Generation at Mid-Ocean Ridges.* Geophys. Monogr., Am. Geophys. Union, 71:183–277.

Ludden, J., and Thompson, G., 1977. An evaluation of the behaviour of REE during weathering of seafloor basalts. *Earth Planet. Sci. Lett.,* 43:85–92.

Machado, N., Ludden, J.N., Brooks, C., and Thompson, G., 1982. Fine scale isotopic heterogeneity in the sub-Atlantic mantle. *Nature,* 295:226–229.

Menzies, M., Blanchard, D., and Jacobs, J., 1977. Rare earth and trace element geochemistry of metabasalts from the Point Sal Ophiolite, California. *Earth Planet. Sci. Lett.,* 37:203–214.

Miyashiro, A., Shido, F., and Ewing, M., 1971. Metamorphism in the Mid-Atlantic Ridge near 24° and 30°N. *Philos. Trans. R. Soc. London A,* 268:589–603.

O'Hara, M.J., 1968. The bearing of phase equilibria studies in synthetic and natural systems on the origin and evolution of basic and ultrabasic rocks. *Earth Sci. Rev.,* 4:69–133.

Presnall, D.C., and Hoover, J.D., 1984. Composition and depth of origin of primary mid-ocean ridge basalts. *Contrib. Mineral. Petrol.,* 87:170–178.

Purdy, G.M., and Detrick, R.S., 1986. Crustal structure of the Mid-Atlantic Ridge at 23°N from seismic refraction studies. *J. Geophys. Res.,* 91:3739–3762.

Reynolds, J.R., 1995. Segment-scale systematics of mid-ocean ridge magmatism and geochemistry [Ph.D. dissert.]. Columbia Univ., Palisades, NY.

Schiffman, P., and Fridleifsson, G.O., 1991. The smectite-chlorite transition in drillhole Nj-15, Nesjavellir geothermal field, Iceland: XRD, BSE and electron microprobe investigation. *J. Metamorph. Geol.,* 9:679–696.

Seyfried, W.E., Jr., and Mottl, M.J., 1982. Hydrothermal alteration of basalt by seawater under seawater-dominated conditions. *Geochim. Cosmochim. Acta,* 46:985–1002.

Shen, Y., and Forsyth, D.W., 1995. Geochemical constraints on initial and final depths of melting beneath mid-ocean ridges. *J. Geophys. Res.,* 100:2211–2237.

Shipboard Scientific Party, 1995. Site 920. *In* Cannat, M., Karson, J.A., Miller, D.J., et al., *Proc. ODP, Init. Repts.,* 153: College Station, TX (Ocean Drilling Program), 45–119.

Sobolev, A.V., and Shimizu, N., 1993. Ultra-depleted primary melt included in an olivine from the Mid-Atlantic Ridge. *Nature,* 363:151–154.

Sparks, J.W., 1995. Geochemistry of the lower sheeted dike complex, Hole 504B, Leg 140. *In* Erzinger, J., Becker, K., Dick, H.J.B., and Stokking, L.B. (Eds.), *Proc. ODP, Sci. Results,* 137/140: College Station, TX (Ocean Drilling Program), 81–98.

Stolper, E., 1980. A phase diagram for mid-ocean ridge basalts: preliminary results and implications for petrogenesis. *Contrib. Mineral. Petrol.,* 78:13–27.

Sullivan, G.E., 1991. Chemical evolution of basalts from 23°N along the mid-Atlantic ridge: evidence from melt inclusions. *Contrib. Mineral. Petrol.,* 106:296–308.

Sun, S.-S., 1980. Lead isotopic study of young volcanic rocks from mid-ocean ridges, ocean islands and island arcs. *Philos. Trans. R. Soc. London A,* 297:409–445.

Sun, S.-S., and McDonough, W.F., 1989. Chemical and isotopic systematics of oceanic basalts: implications for mantle composition and processes. *In* Saunders, A.D., and Norry, M.J. (Eds.), *Magmatism in the Ocean Basins.* Geol. Soc. Spec. Publ. London, 42:313–345.

Takahashi, E., and Kushiro, I., 1983. Melting of a dry peridotite at high pressures and temperatures and basalt magma genesis. *Am. Mineral.,* 68:859–879.

Todt, W., Cliff, R.A., Hanser, A., and Hofmann, A.W., 1984. ^{202}Pb and ^{205}Pb double spike for lead isotopic analyses. *Terra Cognita,* 4:209. (Abstract)

White, W.M., and Hofmann, A.W., 1982. Sr and Nd isotope geochemistry of oceanic basalts and mantle evolution. *Nature,* 296:821–825.

Date of initial receipt: 4 August 1995
Date of acceptance: 22 March 1996
Ms 153SR-030